Journal of the European Ceramic Society **18** (1998) 1331–1337

PII: S0955-2219(98)00062-4
0955-2219/98/$—see front matter

Thermal Stability of $Ce_{1-x}Zr_xO_2$ Solid Solution Powders

Catherine Janvier,[a] Michèle Pijolat,[a]* Françoise Valdivieso,[a] Michel Soustelle[a] and Christophe Zing[b]

[a]Centre SPIN, CRESA, Ecole Nationale Supérieure des Mines, 158 Cours Fauriel, 42023 Saint-Etienne Cedex, France
[b]Centre de Recherches de Rhône-Poulenc, 52 Rue de la Haie Coq, 93308 Aubervilliers Cedex, France

Abstract

High surface area $Ce_{1-x}Zr_xO_2$ powders ($0 < x < 0{\cdot}36$) were annealed at 950°C. The surface area variation versus time of calcination was followed by BET method for all the samples. When the experimental rates of the surface area decrease are plotted versus x, *two extremes are observed: a minimum around 0·09 and a maximum around 0·19. Our previous model involving oxygen and cerium diffusion proposed to interpret the stabilizing effect of zirconium at low content in ceria cannot account for the present experimental rate variations. We propose that the assumption of the ideal behaviour of the solutions is no longer valid when* x *reaches values as high as 0·32 and 0·36. Thus, provided that the $Ce_{1-x}Zr_xO_2$ phases are considered as strictly regular solutions and on the basis of the kinetic model for ceria, it can be shown that the present experimental rate can be interpreted.* © *1998 Elsevier Science Limited. All rights reserved*

1 Introduction

Ceria is an essential component of the three-way catalytic converters for exhausts gas treatment from automobiles.[1,2] The high oxygen-storage capacity of ceria improves the catalytic performances by changing the composition of the automobile fumes, namely storing oxygen during oxidation and releasing it during reduction. The addition of ceria to an alumina support also stabilizes its surface area, which is of great advantage.

It is now well known that the addition of zirconium ions into ceria enhances its oxygen-storage capacity[3] and its thermal stability.[4] For these reasons, the thermal stability of pure[5] and doped[6] ceria has already been investigated. More precisely, we studied the effect of a slight addition of several dopants such as aluminium, silicon or zirconium on the rate of the surface area decrease at high temperature. A kinetic model was proposed to account for the decrease of the surface area in doped ceria. As far as zirconium ions dissolved into ceria are concerned, we found that their inhibiting effect was due to the formation of associated point defects between zirconium (substitutes for cerium ions) and trivalent cerium ions according to the following reaction (we adopt the Kröger's notation[7]):

$$Zr_{Ce}^{x} + Ce_{Ce}' = (Zr, Ce_{Ce}')' \qquad (1)$$

We present here the results obtained when the content in zirconium ions dissolved into ceria is increased at quite high cationic fractions from $x = 0{\cdot}09$ to 0·36 in $Ce_{1-x}Zr_xO_2$. On these ceria–zirconia solid solutions, we performed a kinetic study of their decrease in surface area at 950°C, which results from an increase in crystallite size, and investigated the kinetic influence of the zirconium cationic fraction, x, and the oxygen partial pressure, P_{O2}. The methodology followed is similar to that previously published in our studies on other oxides (γ-Al_2O_3,[7] TiO_2,[8] ZrO_2[9]). It consists of performing the experimental study under suitable conditions in order to obtain the variation of the rate of decrease of the surface area as a function of variables such as, in our case, P_{O2} and x.

We first report (see the Experimental) the characterization conditions of the ceria–zirconia solid solutions and the details of calcination under a controlled atmosphere. Then the variation of the experimental rates of surface area decrease are presented (Results). A kinetic model for the specific surface area variation in solid solutions is then proposed, along with a family of thermodynamic models. Finally we discuss the agreement between the theoretical rate, calculated from the kinetic and the thermodynamic models, and the experimental rate.

2 Experimental

2.1 Samples

$Ce_{1-x}Zr_xO_2$ solid solution powders were provided by Rhône-Poulenc. The initial specific surface areas were of 203, 109, 104, 123, 113, 126 and 119 $m^2 \cdot g^{-1}$ for x equal to 0·00, 0·09, 0·14, 0·19, 0·25, 0·32 and 0·36, respectively.

2.2 Surface area determination

The specific surface area (S_{BET}) of the initial and calcined powders was measured by the BET method using nitrogen adsorption at −196°C on a Micromeritics 2100 E apparatus.

2.3 X-ray diffraction

XRD spectra were recorded on a Siemens D501 diffractometer (CuKα). No demixing of the solid solutions was to be seen either on the initial or the calcined powders, which is in good agreement with the CeO_2–ZrO_2 phase-diagrams usually found in the literature.[10,11]

2.4 Calcination

The samples were calcined in a Pyrox B80 furnace equipped with an alumina tube and a West 2050 regulator. A thermocouple placed inside the alumina tube allowed the measurement of the temperature in the vicinity of the samples. The flowing gas was a mixture of helium, oxygen and carbon dioxide at atmospheric pressure, the composition being adjusted by means of Brooks Shorate 150 flowmeters. The content in water vapour was fixed by flowing the previous mixture over a water bath whose temperature was regulated at −11°C, which corresponds to a partial pressure of water vapour of 0·26 kPa. The partial pressure of oxygen was either 1·7 or 17 kPa. That of carbon dioxide was arbitrarily maintained at 1·3 kPa. Prior to any calcination, the furnace chamber was evacuated, then the gaseous mixture was introduced. The time required to introduce the sample and establish the appropriate calcination conditions did not exceed 9 min. The sample was then removed from the furnace after a calcination time variable between 2 and 14 h. The temperature of calcination was fixed at 950°C, which provided a variation of the samples specific surface areas convenient for the study.

2.5 Experimental rate determination

For each solid solution and each oxygen partial pressure, the kinetic study gives the specific surface area (S) versus the calcination time (t). The experimental values can be fitted with a mathematical function (t being the variable), which, by derivation, gives the experimental rate of surface area decrease versus t. This rate can also be expressed as a function of the specific surface area, which allows the determination of its variation law, for a given value of the specific surface area and for each value of P_{O2}, with x.

As already mentioned in the introduction, this methodology was previously described in studies on other oxides.[7–9]

3 Results

Figure 1 shows the variation of S versus t for a given solid solution ($x = 0{\cdot}32$) at two different oxygen partial pressures. The same curves have been obtained for the other six solid solutions. Obviously from these curves, no influence of the oxygen partial pressure can be seen.

For each kinetic curve, it is possible to determine the parameter A such as

$$S = S_0(1 + At)^n \tag{2}$$

in which S_0 is the initial specific surface area of the solid solutions and n a parameter optimized for each value of x in order to give a good fit for all the experimental conditions. As explained above, the experimental rate of surface area decrease dS/dt can then be obtained by means of a derivation, from the previous equation, as a function of S

$$\frac{dS}{dt} = -nAS_0\left(\frac{S}{S_0}\right)^{\frac{n-1}{n}} \tag{3}$$

From eqn (3) the experimental rate depends on P_{O2}, x (these are a function of A and n) and the specific surface area, S. Thus for a given value of S and P_{O2}, it is possible to obtain the variation of the experimental rate as a function of x, as illustrated in Fig. 2, for each of the two values (1·7 and 17 kPa) of P_{O2}.

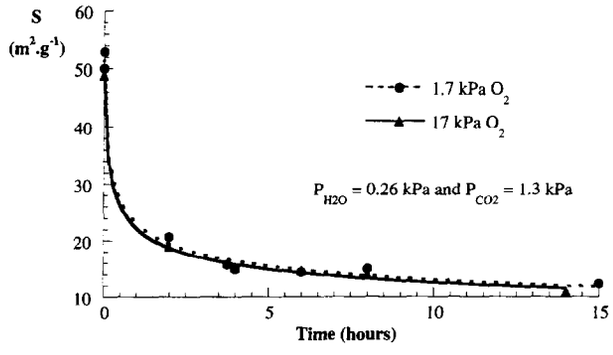

Fig. 1. Surface area (S) versus time of calcination (t) in hours for $Ce_{0{\cdot}68}Zr_{0{\cdot}32}O_2$.

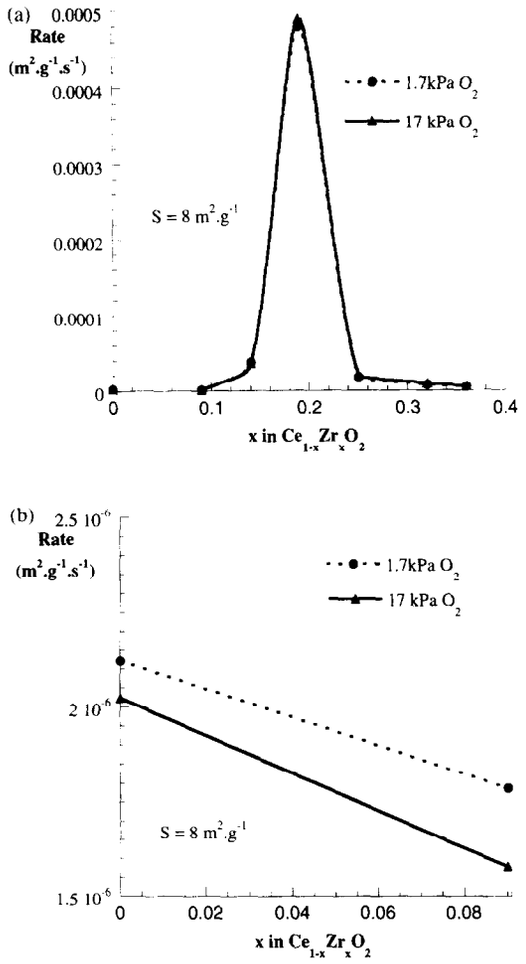

Fig. 2. Experimental rates versus x: (a) x in the 0·00–0·36 range and (b) x in the 0·00–0·09 range.

The experimental rate variation exhibits two extremes: a minimum in the low value of the zirconium content ($0 < x < 0{\cdot}09$) [Fig. 2(b)], already observed in the study of the zirconium-doped ceria,[6] and a maximum ($0{\cdot}14 < x < 0{\cdot}25$) [Fig. 2(a)]. Again, no influence of the oxygen partial pressure can be evidenced.

4 A Model for the Specific Surface Area Variation

Based on the previous study of the crystallite growth in pure[5] and doped ceria,[6] we can propose the following model (Table 1), simply adapted from the ceria system to the particularities of $Ce_{1-x}Zr_xO_2$, in order to account for the decrease of the surface area in the solid solutions. The process takes place in two reactional zones, the convex surfaces of the ceria–zirconia crystallites (denoted $R > 0$) and the neck region between crystallites (denoted $R < 0$). A linear combination of six elementary steps corresponds effectively to the transport from $R > 0$ to $R < 0$ surfaces of a building unit of $Ce_{1-x}Zr_xO_2$, written as follows:

$$(1-x)\underbrace{Ce_{Ce}^{x}}_{R>0} + \underbrace{xZr_{Ce}^{x}}_{R>0} + \underbrace{2O_{O}^{x}}_{R>0} \rightleftarrows (1-x)\underbrace{Ce_{Ce}^{x}}_{R>0} + \underbrace{xZr_{Ce}^{x}}_{R>0} + \underbrace{2O_{O}^{x}}_{R>0} \quad (4)$$

The calculation of the theoretical rate law for the surface area decrease can first be achieved as in the case of doped ceria[6] using the assumption of ideal solutions. It means that the activity coefficient, γi, of each constituent of $Ce_{1-x}Zr_xO_2$ is taken equal to the unit (reference: pure element).

The details of the calculations are the same as those of the zirconium-doped ceria and have already been reported in Ref. 6. In Table 2, we have simply exposed the system of equations to solve in order to calculate the site fractions of the solid solution constituents involved in the elementary steps of Table 1.

It is well known that the diffusion coefficient of oxygen in undoped ceria is more important than that of cerium.[12] When the rate-limiting step of the crystallite growth in solid solutions is supposed to be the cerium vacancies diffusion, which was already the rate-limiting step in zirconium-doped ceria,[6] with the same Brouwer's ($2[V_O^{\circ\circ}] = [(Zr,Ce'_{Ce})']$) and zirconium conservation cases ($x = [Zr_{Ce}^{x}]$), this leads to the following expression of the theoretical rate in solid solutions (since $j_{V_{Ce}^{''''}} = j_{Ce_{Ce}^{x}} + j_{Zr_{Ce}^{x}}$ the cerium vacancies current accounts for the cations diffusion):

$$j_{V_{Ce}^{''''}} = 2^{4/3}\frac{D_{V_{Ce}^{''''}}}{l(r)}K_S K_{Ae}^{-4/3} K_d^{-2/3} x^{-4/3}(1-x)^{-4/3} P_{O_2}^{1/3} \quad (5)$$

This theoretical rate accounts for the stabilizing effect at a low zirconium content (Fig. 3) as we found before[6] but cannot account for our present data and in particular for the maximum in the variation of the experimental rate.

Ceria–zirconia solid solutions seem not to be mixable for all the values of x, but only in the 0·00–0·40 zirconium ranges.[11] Thus the non-adequation between the theoretical and the experimental rates can be attributed to the fact that the assumption of ideal behaviour of the solid solutions is no longer valid when x reaches values as high as 0·32 or 0·36. That is why we have investigated whether a non-ideal thermodynamical model could be more convenient.

The kinetic model presented above takes place at the surface of the oxide particles, so that the thermodynamic model that we are going to propose

Table 1. Modelling of crystallite growth in ceria-zirconia process

Elementary step Kröger's notation	*Quasi-chemical reaction*
1. Oxygen adsorption at $R>0$	$\frac{1}{2}O_2 + V_O^{\circ\circ} + 2Ce'_{Ce} = O_O^x + 2Ce_{Ce}^x$
2. Oxygen diffusion	$V^{\circ\circ}_{O_{R<0}} \rightarrow V^{\circ\circ}_{O_{R>0}}$ and $O^x_{O_{R>0}} \rightarrow O^x_{O_{R<0}}$
3. Vacancies creation at $R<0$	$O_O^x + O_O^x = 2O_O^x + V''''_{Ce} + 2V_O^{\circ\circ}$
4. Oxygen desorption at $R<0$	$O_O^x + 2Ce_{Ce}^x = \frac{1}{2}O_2 + V_O^{\circ\circ} + 2Ce'_{Ce}$
5. Cerium and zirconium diffusion	$V''''_{Ce_{R<0}} \rightarrow V''''_{Ce_{R>0}}$ and $(1-x)Ce^x_{Ce_{R>0}} \rightarrow (1-x)Ce^x_{Ce_{R<0}}$ and $xZr^x_{Ce_{R>0}} \rightarrow xZr^x_{Ce_{R<0}}$
6. Vacancies annihilation at $R>0$	$2V_O^{\circ\circ} + V''''_{Ce} = 0$

Table 2. System of equations to resolve in order to calculate the site fractions of the constituents in ceria-zirconia solid solutions

Equation or equilibrium to consider	
Charge balance equation	$2[V_O^{\circ\circ}] = [Ce'_{Ce}] + [(Zr, Ce'_{Ce})'] + 4[V''''_{Ce}]$
Zirconium conservation equation	$x = [Zr^x_{Ce}] + [(Zr, Ce'_{Ce})']$
Cerium sites conservation equation	$1 = [Ce^x_{Ce}] + [Zr^x_{Ce}] + [Ce'_{Ce}] + 2[(Zr, Ce'_{Ce})'] + [V''''_{Ce}]$
Formation equilibrium of (Zr,Ce'_{Ce})	$K_{Ae} = \frac{\gamma_{Zr_A}[(Zr,Ce'_{Ce})]}{\gamma_{Zr}[Zr^x_{Ce}]\gamma_{Ce'}[Ce'_{Ce}]}$
Equilibrium between O_2 and $Ce_{1-x}Zr_xO_2$	$K_d = \frac{\gamma^2_{Ce'}[Ce'_{Ce}]^2\gamma_{V_O^{\circ\circ}}[V_O^{\circ\circ}]P_{O_2}^{\frac{1}{2}}}{\gamma^2_{Ce}[Ce^x_{Ce}]^2}$
Equilibrium of vacancies creation	$K_S = \gamma^2_{V_O^{\circ\circ}}[V_O^{\circ\circ}]^2\gamma_{V''''_{Ce}}[V''''_{Ce}]$

attempts to describe the ceria–zirconia solid solutions on the surface (no assumption on the bulk behaviour has to be done).

$Ce_{1-x}Zr_xO_2$ can be described with the following structural constituents: $Ce_{Ce}{}^x$, $Zr_{Ce}{}^x$, $O_O{}^x$, Ce'_{Ce}, (Zr,Ce'_{Ce}), $V^{\circ\circ}{}_O$ and $V''''{}_{Ce}$. These can be arranged into two sublattices: an anionic one composed of $O_O{}^x$ and $V^{\circ\circ}{}_O$ and a cationic one composed of $Ce_{Ce}{}^x$, $Zr_{Ce}{}^x$, Ce'_{Ce}, $(Zr,Ce'_{Ce})'$ and $V''''{}_{Ce}$.

We suppose that the anionic sublattice has an ideal behaviour ($\gamma O_O{}^x = 1$ and $\gamma V^{\circ\circ}{}_O = 1$) and that

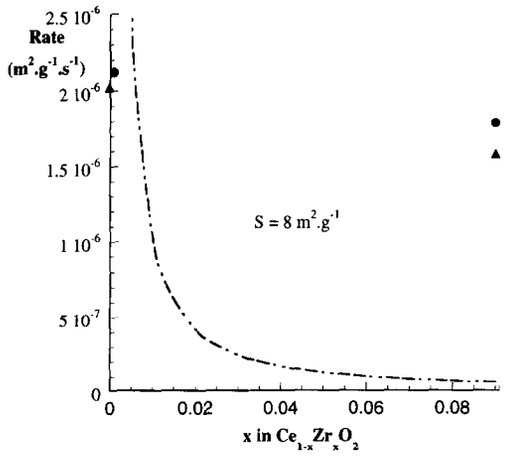

Fig. 3. Theoretical rate variation in the x range 0·00–0·09 on the assumptions of cerium vacancies diffusion limiting step and ideal behaviour of the solutions, the experimental rates being represented at two different oxygen partial pressures: (●) 1·7 kPa and (▲) 17 kPa.

the cationic sublattice has a *partially strictly regular* behaviour. This means that at least two of the activity coefficients of the cationic sublattice constituents are different from 1. From this point, we will refer to solid solutions with such a behaviour as partially strictly regular solutions, which means that they have all the properties of a strictly regular solution.[13] Thus the excess molar Gibbs energy of the partially strictly regular solution[14] is defined by:

$$G^m_{xs} = \sum_{i=1}^{n}\sum_{j=i+1}^{n} \lambda_{ij}x_ix_j \qquad (6)$$

where λ_{ij} are the interaction parameters between the i and j constituents (independent of x and temperature, T), xi and xj are their site fractions on the cationic sublattice, n the number of the constituents in the solution with an activity coefficient different from 1.

Since $V''''{}_{Ce}$ is present in $Ce_{1-x}Zr_xO_2$ at an extremely low concentration, we could keep its activity coefficient equal to 1. Thus six pseudo-binaries (i.e. six different kind of models of partially strictly regular solutions with two of the cationic constituents having an activity coefficient different from 1 and considered as the major cationic elements) and four pseudo-ternaries are possible. They are listed in Table 3.

Table 3. Expression of the rate deduced from the model of ceria-zirconia crystallite growth in the case of a cerium vacancies diffusion limiting step, in the zirconium conservation ($x=[Zr_{Ce}^{x}]$), Brouwer's ($2[V^{\circ\circ}_{O}]=[(Zr,Ce'_{Ce})']$ and cerium sites conservation ($[Ce_{Ce}^{x}]+[Zr_{Ce}^{x}]=1$) cases, the thermodynamic model describing the solutions being: (a) a pseudo-binary and (b) a pseudo-ternary one

Pseudo-binary models	*Relation from the Gibbs-Duhem equation*	*Theoretical rate* $j_{V''''_{Ce}}$
(1) Ce_{Ce}^{x} and Zr_{Ce}^{x}	$[Ce_{Ce}^{x}]+[Zr_{Ce}^{x}]=Cst$	$2^{4/3}\frac{D_{V''''_{Ce}}}{l(r)}K_S K_{Ae}^{-4/3}K_d^{-2/3}x^{-4/3}(1-x)^{-4/3}P_{O_2}^{1/3}$ $\exp\left[-\frac{4}{3}\frac{\lambda_{Ce/Zr}}{RT}(2x^2-2x+1)\right]$
(2) Ce_{Ce}^{x} and Ce'_{Ce}	$[Ce_{Ce}^{x}]+[Ce'_{Ce}]=Cst$	Not allowed
(3) Ce_{Ce}^{x} and (Zr,Ce'_{Ce})	$[Ce_{Ce}^{x}]+[(Zr,Ce'_{Ce})']=Cst$	Not allowed
(4) Zr_{Ce}^{x} and (Zr,Ce'_{Ce})	$[Zr_{Ce}^{x}]+[(Zr,Ce'_{Ce})']=Cst$	Not alllowed
(5) Zr_{Ce}^{x} and Ce'_{Ce}	$[Zr_{Ce}^{x}]+[Ce'_{Ce}]=Cst$	Not allowed
(6) (Zr,Ce'_{Ce}) and Ce'_{Ce}	$[(Zr,Ce'_{Ce})']+[Ce'_{Ce}]=Cst$	Not allowed
Pseudo-ternary models	*Relation from the Gibbs-Duhem equation*	*Theoretical rate* $j_{V''''_{Ce}}$
(1) Ce_{Ce}^{x}, Zr_{Ce}^{x} and Ce'_{Ce}	$[Ce_{Ce}^{x}]+[Zr_{Ce}^{x}]+[Ce'_{Ce}]=Cst$	Not allowed
(2) Ce_{Ce}^{x}, Zr_{Ce}^{x} and (Zr,Ce'_{Ce})	$[Ce_{Ce}^{x}]+[Zr_{Ce}^{x}]+[(Zr,Ce'_{Ce})']=Cst$	$2^{4/3}\frac{D_{V''''_{Ce}}}{l(r)}K_S K_{Ae}^{-4/3}K_d^{-2/3}x^{-4/3}(1-x)^{-4/3}P_{O_2}^{1/3}$ $\exp\left[-\frac{4}{3}\frac{\lambda_{Ce/Zr}}{RT}x^2-\frac{4}{3RT}(\lambda_{Ce/Zr_A}-\lambda_{Ce/Zr}-\lambda_{Zr/Zr_A})\right.$ $\left.x-\frac{4}{3RT}(\lambda_{Ce/Zr}-\lambda_{Ce/Zr_A})\right]$
(3) Ce_{Ce}^{x}, Ce'_{Ce} and (Zr,Ce'_{Ce})	$[Ce_{Ce}^{x}]+[Ce'_{Ce}]+[(Zr,Ce'_{Ce})']=Cst$	Not allowed
(4) Ce'_{Ce}, Zr_{Ce}^{x} and (Zr,Ce'_{Ce})	$[Ce'_{Ce}]+[Zr_{Ce}^{x}]+[(Zr,Ce'_{Ce})']=Cst$	Not allowed

As in all solutions, the Gibbs–Duhem relation must be respected. It leads to the following relation between the molar fractions of the constituents with an activity coefficient different from 1:

$$\sum_{i=1}^{n} x_i = \text{Constant} \tag{7}$$

There must be a complete compatibility between, on the one hand the approximations used in the charge balance, the zirconium conservation and the cerium sites conservation equations, and on the other hand the relation (7), obtained for each thermodynamic model chosen for describing the ceria–zirconia solid solutions. Hence the restrictions on the possible pseudo-binaries and pseudo-ternaries that are given in Table 3.

From these considerations it follows that each activity coefficient different from 1, γ_i (i representing any of the constituents of the cationic sublattice with an activity coefficient different from 1), can be expressed as a function of x, λ_{ij} and T, since the excess molar partial Gibbs energy, μ_{xs}, is:

$$\mu_{xs} = RT\ln\gamma_i = \left(\frac{\partial G_{xs}}{\partial n_i}\right)_{T,P,N_{j\neq 1}} \tag{8}$$

The site fractions of each constituent of the solid solutions can then be readily expressed as a function of x, λ_{ij} and T by resolving the system of equations exposed in Table 2, for each thermodynamic model allowed for describing the ceria–zirconia solid solutions.

From these various thermodynamic models, we can obtain the theoretical rate of surface area decrease and compare it with the experimental one according to eqn (5) in which the expression of activity coefficients will appear.

5 Discussion

The expression of the theoretical rates for each allowed thermodynamic model are given in the third column of Table 3.

In Fig. 4, the experimental rates obtained for 17 kPa of oxygen have been fitted to the theoretical law obtained in the case of the pseudo-binary Ce_{Ce}^{x} and Zr_{Ce}^{x}, with $\lambda_{Ce/Zr}$ and the thermodynamic constants K_i as adjusted parameters. As we can see, the theoretical rate exhibits two extremes: a minimum below 0·09 and a maximum fixed at 0·50, which is not surprising due to the symmetry of the pseudo-binary corresponding model. The model (1) of Table 3 is therefore not acceptable.

In Fig. 5, the experimental rates at 17 kPa of oxygen (full line, triangular points) are fitted to the theoretical law obtained in the case of the pseudo-ternary Ce_{Ce}^{x}, Zr_{Ce}^{x} and $(Zr,Ce'_{Ce})'$ [model (2) Table 3], in which $\lambda_{Ce/Zr}$, $\lambda_{Ce/ZrA}$, $\lambda_{Zr/ZrA}$ and K_i are the adjusted parameters. The theoretical rate

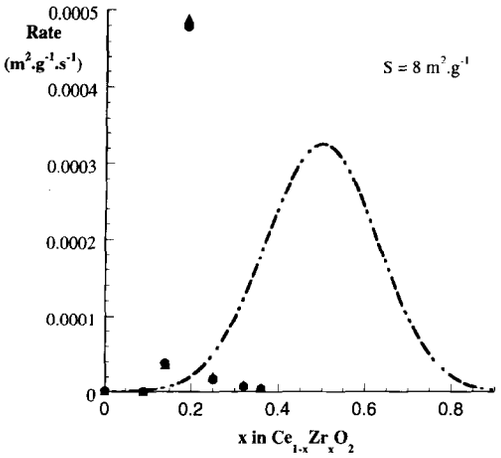

Fig. 4. Theoretical rate variation on the assumptions of cerium vacancies diffusion limiting step and a pseudo-binary model of Ce_{Ce}^{x} and Zr_{Ce}^{x} for describing the solutions, the experimental rates being represented at two different oxygen partial pressures: (●) 1·7 kPa and (▲) 17 kPa.

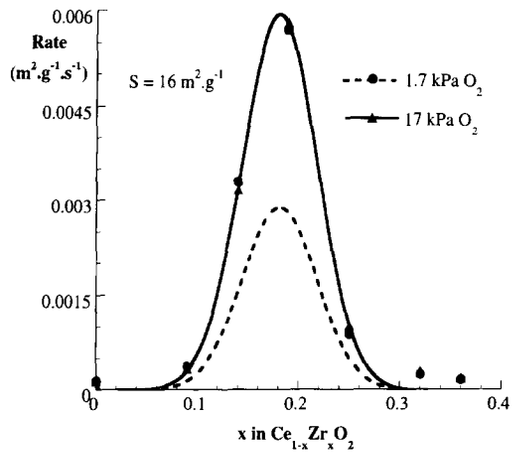

Fig. 5. Theoretical rate variation at two different oxygen partial pressures on the assumptions of cerium vacancies diffusion limiting step and a pseudo-ternary model of Ce_{Ce}^{x} Zr_{Ce}^{x} and $(Zr,Ce'_{Ce})'$ for describing the solutions.

Table 4. Expression of the rate deduced from the model of ceria-zirconia crystallite growth in the case of a mixed diffusion of cations and anions, in the zirconium conservation ($x=[Zr_{Ce}^{x}]$), Brouwer's ($2[V^{\circ\circ}_{O}]=[(Zr,Ce'_{Ce})']$ and cerium sites conservation ($[Ce_{Ce}^{x}]+[Zr_{Ce}^{x}]=1$) cases, the thermodynamic model describing the solutions being the pseudo-ternary one of Ce_{Ce}^{x}, Zr_{Ce}^{x} and $(Zr,Ce'_{Ce})'$

Pseudo-ternary model	*Theoretical rate* j_{Mixed}
Ce_{Ce}^{x}, Zr_{Ce}^{x} and $(Zr,Ce'_{Ce})'$	$j_O = 3\frac{D_O}{l(r)}2^{-2/3}K_d^{1/3}K_{Ae}^{2/3}P_{O_2}^{-1/6}x^{2/3}(1-x)^{2/3}\frac{\exp\left[\frac{2}{3RT}\lambda_{Ce/Zr}x^2+\frac{2}{3RT}(\lambda_{Ce/Zr_A}-\lambda_{Ce/Zr}-\lambda_{Zr/Zr_A})x+\frac{2}{3RT}(\lambda_{Ce/Zr}-\lambda_{Ce/Zr_A})\right]}{1+2\frac{D_O}{D_{Ce}}K_{Ae}x\exp\left[\frac{1}{RT}(\lambda_{Ce/Zr_A}-\lambda_{Ce/Zr}-\lambda_{Zr/Zr_A})x+\frac{1}{RT}(\lambda_{Ce/Zr}-\lambda_{Ce/Zr_A})\right]}$
	$j_{V''''_{Ce}} = 2^{4/3}\frac{D_{V''''_{Ce}}}{l(r)}K_S K_{Ae}^{-4/3}K_d^{-2/3}x^{-4/3}(1-x)^{-4/3}P_{O_2}^{1/3}$ $\exp\left[-\frac{4}{3}\frac{\lambda_{Ce/Zr}}{RT}x^2-\frac{4}{3RT}(\lambda_{Ce/Zr_A}-\lambda_{Ce/Zr}-\lambda_{Zr/Zr_A})x-\frac{4}{3RT}(\lambda_{Ce/Zr}-\lambda_{Ce/Zr_A})\right]$
	$j_{Mixed}=\frac{j_O j_{V''''_{Ce}}}{j_O+j_{V''''_{Ce}}}$

exhibits two extremes: a minimum at 0·02 and a maximum whose position can be adjusted at 0·18. It can be seen that this model fits very well the dots. However, the model predicts an influence of the oxygen partial pressure as $P_{O2}^{1/3}$ on the rate of the surface area decrease, which is not in agreement with our experimental results (no influence of P_{O2} could be evidenced). This is illustrated in Fig. 5 by the dotted line, representing the corresponding theoretical rate at 1·7 kPa, deduced from the rate for 17 kPa of oxygen. This shows that there is no agreement with the data.

If now we consider that the theoretical rate is given by the mixed diffusion of cations and anions in the steady state approximation,[6] j_{Mixed}, according to:

$$j_{Mixed}=\frac{j_O j_{V''''_{Ce}}}{j_O+j_{V''''_{Ce}}} \qquad (10)$$

where j_O is the diffusion current of oxygen calculated on the assumption of the oxygen diffusion limiting step, and $j_{V''''_{Ce}}$ is the diffusion current of the cerium vacancies, we obtain the expression of Table 4. In Fig. 6, we fitted the experimental rates at 17 kPa of oxygen (full line, triangular points) with this expression, with $\lambda_{Ce/Zr}$, $\lambda_{Ce/ZrA}$, $\lambda_{Zr/ZrA}$, and K, as adjusted parameters. The theoretical rate exhibits again two extremes: a minimum at 0·02 and a maximum whose position is adjustable to 0·17. This model still accounts for the variation of the experimental rates versus x. The dotted line in Fig. 6 represents this calculated rate for 1·7 kPa oxygen pressure. We can see that now the theoretical rates at 17 and 1·7 kPa are very close. The dotted curve provides then a good prediction for the experimental rate points at 1·7 kPa (round points).

The fit of the experimental rates by the pseudo-ternary model (2) of Table 3 gives the values of λ_{ij}, interaction parameters in the ceria-zirconia solid solutions. The values giving the best agreement are:

(a) $\lambda_{Ce/Zr}=174$ kJ/mol

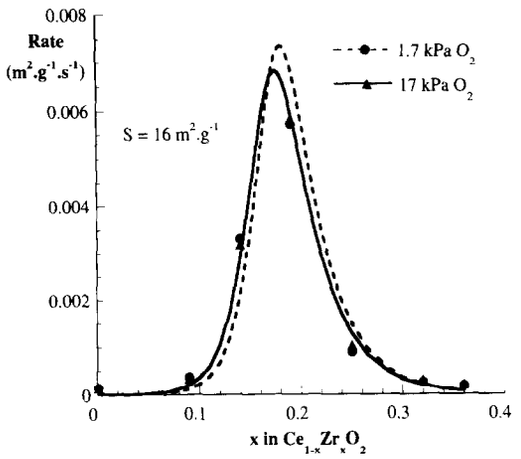

Fig. 6. Theoretical rate variation at two different oxygen partial pressures on the assumptions of a mixed diffusion of anions and cations and a pseudo-ternary model of Ce_{Ce}^{x}, Zr_{Ce}^{x} and $(Zr,Ce'_{Ce})'$ for describing the solutions.

(b) $\lambda_{Ce/ZrA} = 183\,kJ/mol$
(c) $\lambda_{Zr/ZrA} = 508\,kJ/mol$

but they are not extremely precise since the positions of both the minimum and the maximum on the rate curve are not well defined from the experimental data.

6 Conclusion

We studied the rate of surface area decrease of several $Ce_{1-x}Zr_xO_2$ samples at 950°C. We found that, when plotted versus x, the experimental rate (deduced from the kinetic curves) exhibited two extremes: a minimum around 0·09 and a maximum around 0·19. No influence of the oxygen partial pressure could be evidenced.

Using a kinetic model based on previous kinetic modelling of crystallite growth in undoped and doped ceria and considering various thermodynamic models of partially strictly regular solutions, the site fractions of each constituent of $Ce_{1-x}Zr_xO_2$ along with the expressions of theoretical rates can be expressed as a function of the zirconium content, the temperature and the interaction parameters of the solution. The experimental results are then discussed on the basis of a cerium vacancies diffusion or a mixed diffusion combined with a pseudo-binary or a pseudo-ternary thermodynamic model for the solid solutions.

It appears that the experimental rates variation is best represented when the theoretical rate is calculated on the assumptions of a mixed diffusion of anions and cations in the kinetic model and a thermodynamic model for the cationic sublattice of a partially strictly regular solution of Ce_{Ce}^{x}, Zr_{Ce}^{x} and and $(Zr,Ce'_{Ce})'$. Since the crystallite growth takes place at the surface of the oxides particles, this thermodynamic model describes the ceria–zirconia solid solutions on their surface as well. The bulk behaviour in terms of thermodynamic behaviour is still to be studied.

References

1. Nunan, L. G., Robota, H. J., Cohn, M. J. and Bradley, S. A., Physicochemical properties of Ce-containing three-way catalysts and the effect of Ce on catalyst activity. *J. Catal.*, 1992, **133**, 309–324.
2. Diwell, A. F., Rajaram, R. R., Shaw, H. A. and Truex, T. L., The role of ceria in three-way catalysts. *Stud. Surf. Sci. Catal.*, 1991, **71**, 139–152.
3. Balducci, G., Fornasiero, P., Di Monte, R., Kaspar, L., Meriani, S. and Graziani, M., An unusual promotion of the redox behaviour of CeO_2–ZrO_2 solid solutions upon sintering at high temperatures. *Catal. Lett.*, 1995, **33**, 193–200.
4. Sauvion, G. N. and Caillod, J., Rhône-Poulenc, French Patent, 2584388, 1985.
5. Pijolat, M., Prin, M., Soustelle, M. and Nortier, P., Evolution de la texture d'un oxyde de cérium à haute temperature. II. Influence de la vapeur d'eau, de l'oxygène et du dopage aux ions Si^{4+} et Al^{3+}. *J. Chim. Phys.*, 1994, **91**, 51–62.
6. Pijolat, M., Prin, M., Soustelle, M., Touret, O. and Nortier, P., Thermal stability of doped ceria: experiment and modelling. *J. Chem. Soc. Faraday Trans.*, 1995, **91**, 193–200.
7. Pijolat, M., Dauzat, M. and Soustelle, M., Influence of water vapor and additives on the surface area stability of γ-Al_2O_3. *Solid State Ionics*, 1992, **50**, 31–41.
8. Hébrard, J.L., Nortier, P., Pijolat, M. and Soustelle, M., Initial sintering of submicrometer titania-anatase powder. *J. Am. Ceram. Soc.*, 1990, **73**, 79-84; Gruy, F. and Pijolat, M., Kinetics of anatase TiO_2 surface area reduction in a mixture of HCl, H_2O and O_2. *J. Am. Ceram. Soc.*, 1992, **75**, 657–662 and 663–666.
9. Méthiviers, A. and Pijolat, M., Thermal stability of zirconia as a catalyst support: kinetics and modelling. *J. Catal.*, 1993, **139**, 329–337.
10. Yashima, M., Takashina, H., Kakihana, M. and Yoshimura, M., Assessment of the phase diagramm in the ZrO_2–CeO_2 system. Rep. *Res. Lab. Eng. Mater., Tokyo Inst. Technol.*, 1994, **19**, 41–50.
11. Yashima, M., Arashi, H., Kakihana, M. and Yoshimura, M., Raman scattering study of cubic–tetragonal phase transition in $Zr_{1-x}Ce_xO_2$ solid solution. *J. Am. Ceram. Soc.*, 1994, **77**, 1067–1071.
12. Panlener, R. J., Blumenthal, R. N. and Gamier, J. E., A thermodynamic study of nonstoicheometric cerium dioxide. *J. Phys. Chem. Solids*, 1975, **36**, 1213–1222.
13. Hildebrand, J. H., Solubility. XII. Regular solutions. *J. Amer. Chem. Soc.*, 1929, **51**, 66–80.
14. Soustelle, M., *Modélisation macroscopique des transformations physico-chimiques*, ed. Masson, Paris, 1990, pp. 84–86.